

Reversibly Cross-Linked Polyplexes Enable Cancer-Targeted Gene Delivery via Self-Promoted DNA Release and Self-Diminished Toxicity

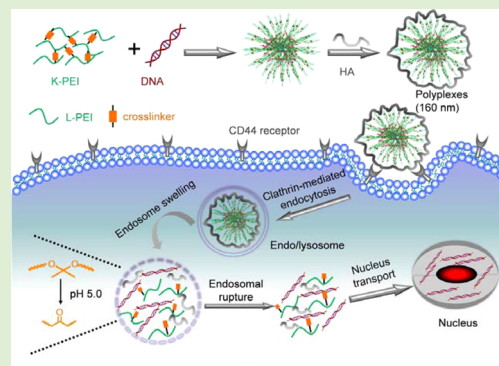
Hua He,[†] Yugang Bai,[‡] Jinhui Wang,[§] Qiurong Deng,[§] Lipeng Zhu,[§] Fenghua Meng,[†] Zhiyuan Zhong,^{*,†} and Lichen Yin^{*,§}

[†]Biomedical Polymers Laboratory and Jiangsu Key Laboratory of Advanced Functional Polymer Design and Application, College of Chemistry, Chemical Engineering and Materials Science, and [§]Jiangsu Key Laboratory for Carbon-Based Functional Materials and Devices, Institute of Functional Nano and Soft Materials (FUNSOM), Soochow University, Suzhou 215123, People's Republic of China

[‡]Department of Chemistry, University of Illinois at Urbana–Champaign (UIUC), 600 South Mathews Avenue, Urbana, Illinois 61801, United States

Supporting Information

ABSTRACT: Polycations often suffer from the irreconcilable inconsistency between transfection efficiency and toxicity. Polymers with high molecular weight (MW) and cationic charge feature potent gene delivery capabilities, while in the meantime suffer from strong chemotoxicity, restricted intracellular DNA release, and low stability in vivo. To address these critical challenges, we herein developed pH-responsive, reversibly cross-linked, polyetheleneimine (PEI)-based polyplexes coated with hyaluronic acid (HA) for the effective and targeted gene delivery to cancer cells. Low-MW PEI was cross-linked with the ketal-containing linker, and the obtained high-MW analogue afforded potent gene delivery capabilities during transfection, while rapidly degraded into low-MW segments upon acid treatment in the endosomes, which promoted intracellular DNA release and reduced material toxicity. HA coating of the polyplexes shielded the surface positive charges to enhance their stability under physiological condition and simultaneously reduced the toxicity. Additionally, HA coating allowed active targeting to cancer cells to potentiate the transfection efficiencies in cancer cells in vitro and in vivo. This study therefore provides an effective approach to overcome the efficiency-toxicity inconsistency of nonviral vectors, which contributes insights into the design strategy of effective and safe vectors for cancer gene therapy.



INTRODUCTION

Gene therapy affords a promising and efficient way to treat congenital and acquired diseases by delivering generic materials into target cells to promote or rectify the expression of specific genes.^{1,2} While viral vectors afford high transfection efficiencies due to their innate ability to enter and utilize transcription machinery of host cells, they suffer from inherent immunogenicity, carcinogenicity, and insertional mutagenesis.³ Therefore, the clinical application of viral vectors is greatly hindered. Nonviral vectors, exemplified by cationic polymers and lipids, are characterized by minimal immunogenicity and carcinogenicity and, thus, serve as ideal alternatives to viral vectors toward clinical gene therapy.^{4,5} As an important category of nonviral vectors, cationic polymers (also termed as polycations) are capable of condensing the anionic nucleic acids into nanocomplexes and thus facilitating their intracellular delivery. Despite such desired properties, the inconsistency between the transfection efficiency and chemotoxicity of polycations always remains as a critical challenge against their wide utilities.

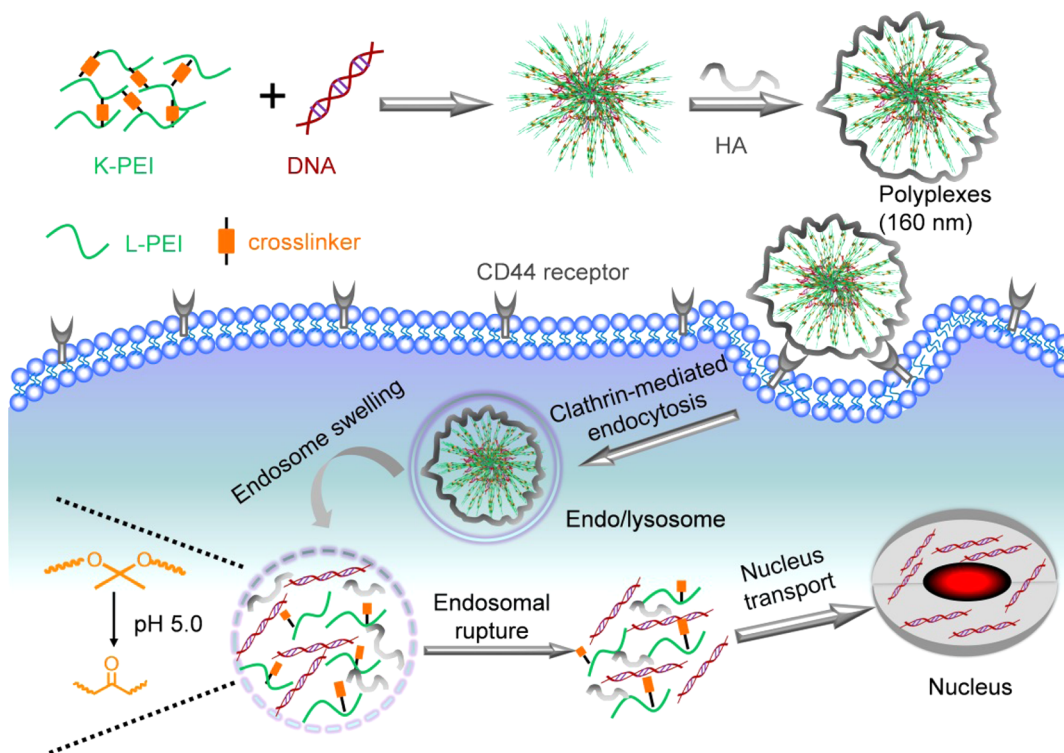
The first major inconsistency is related to the molecular weight (MW) of polycations. Particularly, polymers with high MW afford stronger DNA condensation capacities than their low-MW analogues and thus mediate stronger intracellular gene delivery capabilities and transfection efficiencies.^{6,7} However, the excessively strong binding affinity toward nucleic acids will impede the intracellular release of gene cargos, which will otherwise fight against effective gene transfection.^{8,9} Additionally, high-MW polymers will induce stronger post-transfection cytotoxicity due to the higher amount of contact points with cell membranes, especially at high polymer concentrations or after long-term incubation.¹⁰ The appreciable chemotoxicity of polymers not only raises safety issues against clinical applications, but inversely hampers the transfection efficiency as well due to remarkable loss of cell viability and function.¹¹ To address such

Received: February 8, 2015

Revised: March 7, 2015

Published: March 10, 2015

Scheme 1. Formation and Intracellular Kinetics of K-PEI/HA/DNA Polyplexes, Including DNA Condensation by K-PEI, Followed by HA Coating via Electrostatic Interaction, Cell Uptake of Polyplexes via HA Receptor- and Clathrin-Mediated Endocytosis, Acid-Triggered De-Cross-Linking of K-PEI, and Dissociation of Polyplexes, Endosomal Rupture, and Cytoplasmic Release of DNA via PEI-Assisted “Proton Sponge” Effect, and Nucleus Transport of DNA towards Gene Transcription

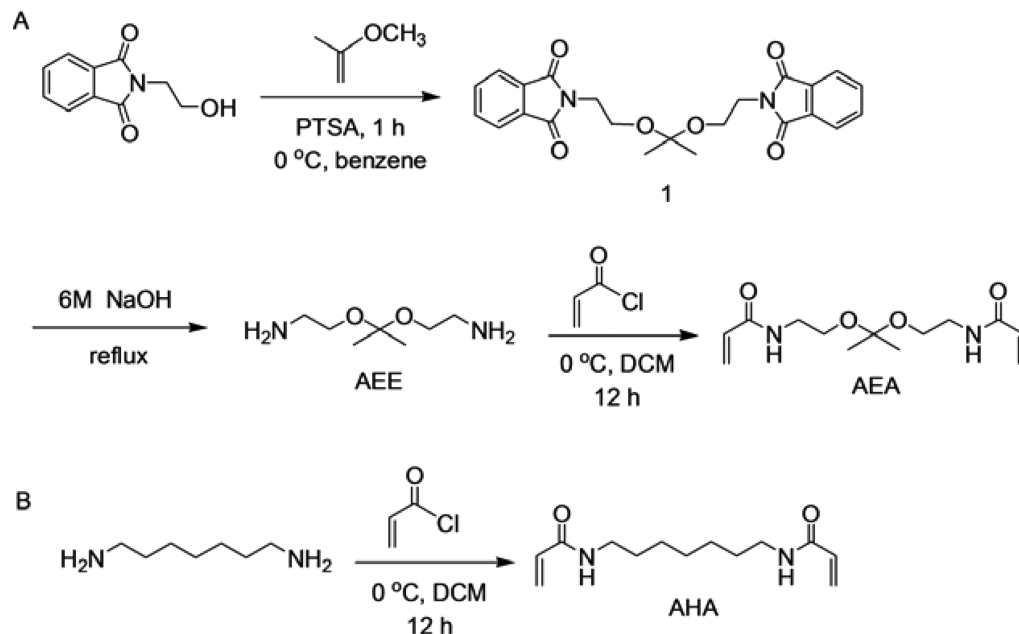


critical challenge, it is thus highly demanded to develop a vector that possesses sufficient MW and charge density during the transfection process to overcome the cellular barriers against gene delivery while can be triggered to instantaneously degrade into small segments at the post-transfection state, such that “on-demand” gene release can be allowed and material toxicity can be diminished.¹²

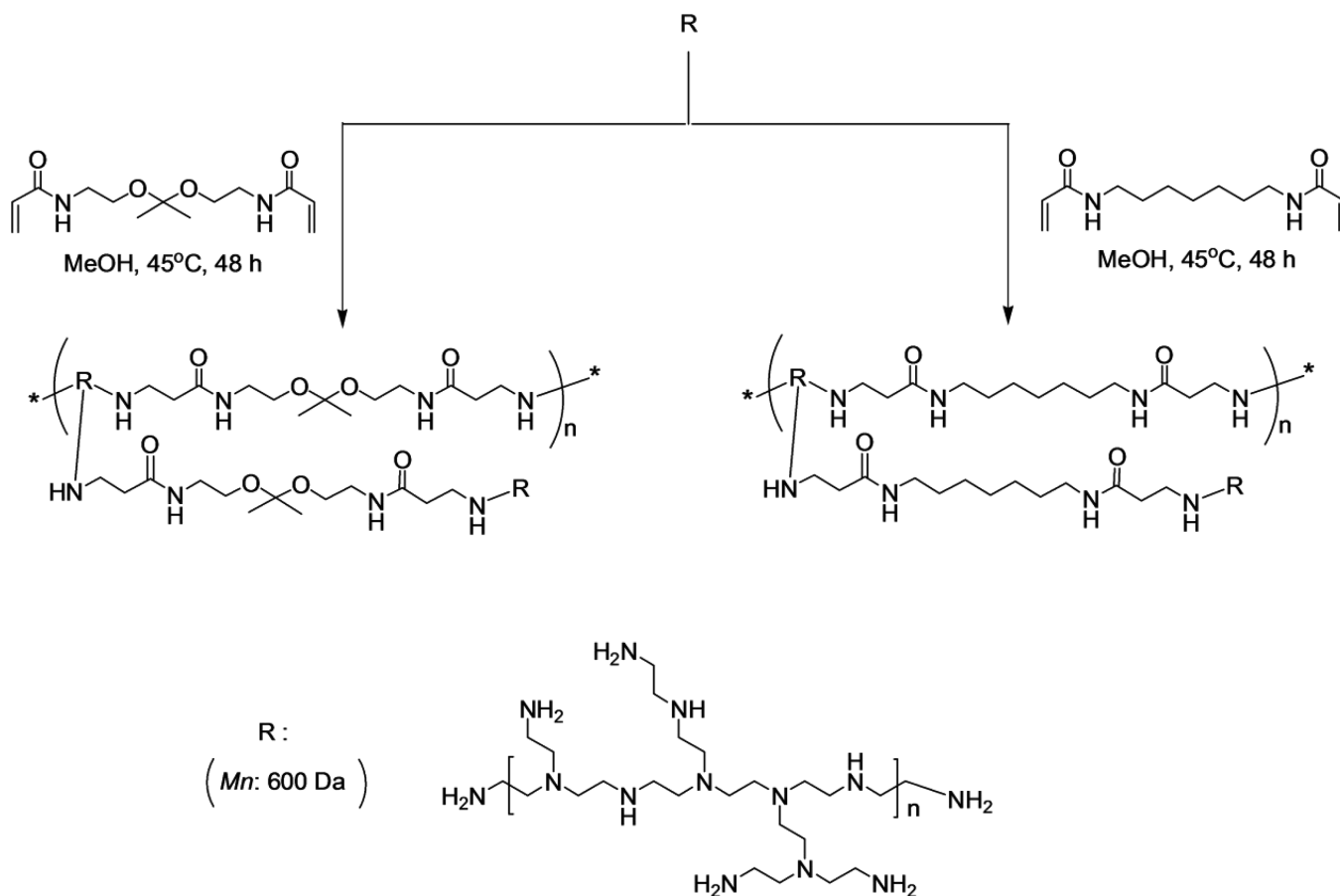
Another critical inconsistency is associated with the cationic charge density of polyplexes. While the positive surface charges on polyplexes feature effective binding to the negatively charged cell membrane and accordingly facilitate the cellular internalization, the excessive cationic charge density may at the meantime induce notable damage to the cell membranes especially at high concentrations or after long-term incubation.^{13,14} Additionally, upon systemic administration, the circulating polyplexes are prone to adsorb negatively charged serum proteins via electrostatic interaction,^{15,16} resulting in nanoparticle aggregation and recognition by the reticuloendothelial system (RES) that ultimately leads to remarkable entrapment in RES organs (such as liver and spleen) yet very little accumulation in tumors.^{15–17} As such, the in vivo application of polycations is greatly hindered. PEGylation of polycations serves as the most widely used strategy to improve their safety as well as serum stability because the neutral and hydrophilic PEG molecules create a hydrophilic corona on polyplex surfaces to shield the positive charges and sterically hinder the binding of blood components.^{18–20} However, PEGylated polycations often suffer from significantly reduced gene transfection capabilities.^{21–23} Such inconsistency thus highlights alternative strategies that can address the charge-associated safety and stability issues of polycations without compromising the transfection efficiencies.

With the attempt to address the aforementioned critical challenges associated with polycation-mediated gene delivery, we herein developed pH-responsive, reversibly cross-linked, polyethyleimine (PEI)-based polyplexes coated with hyaluronic acid (HA) for the effective and targeted gene delivery to cancer cells in vitro and in vivo. PEI is a widely utilized transfection reagent because of its potent pH buffering capability to mediate effective endosomal escape via the “proton sponge” effect,^{24–27} which, however, also suffers from the MW-dependent efficiency-toxicity inconsistency. Particularly, commercially available branched PEI 25 kDa is a golden standard reagent with high transfection efficiency, while at the meantime, induces notable cytotoxicity due to cell membrane disruption followed by induction of apoptosis via destabilization of mitochondrial membranes. On the contrary, low-MW PEI (MW < 2 kDa) demonstrates negligible cytotoxicity yet much lower transfection ability. To solve this problem, low MW branched PEI (L-PEI, 600 Da) was cross-linked via a pH-labile ketal linker to obtain PEI with high MW and cationic charge density (K-PEI). We hypothesized that such reversibly cross-linked PEI would afford greatly enhanced DNA condensation capability to promote the intracellular internalization of DNA cargoes;^{28–30} upon treatment with internal acid triggers in the endolysosome (pH ~ 5.0), it could be instantaneously degraded into low-MW pieces upon cleavage of the ketal bonds such that the intracellular DNA release could be enhanced to potentiate the gene transfection efficiency and the post-transfection material toxicity can also be largely diminished (Scheme 1).³¹ While other cross-linkers such as disulfides³⁰ have been used to cross-link L-PEI that undergoes redox-triggered disulfide cleavage by cytoplasmic glutathione (GSH), the pH-responsive ketal-based cross-linking could allow rapid degradation of PEI in the endosomes directly upon cellular

Scheme 2. Synthesis of AEA (A) as the pH-Responsive Cross-Linker and its Nonresponsive Analogue AHA (B)



Scheme 3. Synthesis of pH-Responsive PEI (K-PEI) and Its Nonresponsive Analogue NK-PEI



internalization such that material toxicity could be diminished at an earlier stage. Hyaluronic acid (HA) as a natural anionic polysaccharide was further selected to coat the K-PEI/DNA polyplexes because it can not only reduce the surface cationic charge of polyplexes but also can recognize the abundant HA receptors (such as CD44) on cancer cells.³² We thus

hypothesized that the stability as well as cell tolerability of polyplexes could be greatly enhanced. Because HA was capable of targeting cancer cells to potentiate the HA-receptor-mediated endocytosis,^{33,34} we also hypothesized that HA coating would strengthen the cancer-targeted gene delivery efficiency of K-PEI instead of diminishing the transfection efficiency as a result of

cationic charge shielding (Scheme 1). To prove these design strategies, we mechanistically evaluated the pH-responsive gene delivery properties by probing the acid-triggered polymer degradation, DNA release, transfection efficiency, and cytotoxicity. The effect of HA-mediated cancer targeting on gene transfection as well as cytotoxicity was also investigated.

EXPERIMENTAL SECTION

Materials. Branched PEI (bPEI) with MW of 25 kDa (H-PEI) and 600 Da (L-PEI), *N*-(2-hydroxyethyl)-phthalimide, 2-methoxy propene, *p*-toluenesulfonic acid, and wortmannin were purchased from J&K (Beijing, China). Hyaluronic acid (HA) with MW of 35 kDa was purchased from Shangdong Freda Biopharm Co. Ltd. Acryloyl chloride was purchased from Energy Chemical (Shanghai, China). 1,7-Diaminoheptane, chlorpromazine, and genistein were purchased from TCI (Shanghai, China). Methyl- β -cyclodextrin was purchased from Aladdin (Shanghai, China). YOYO-1 was purchased from Invitrogen (Carlsbad, CA, U.S.A.).

HeLa (human cervix adenocarcinoma cells), 3T3-L1 (mouse embryonic fibroblasts), B16F10 (mouse melanoma cells), and RAW 264.7 (mouse monocyte macrophages) were purchased from the American Type Culture Collection (Rockville, MD, U.S.A.) and were cultured in Dulbecco's modified Eagle medium (DMEM; Gibco, Grand Island, NY, U.S.A.) containing 10% fetal bovine serum.

Male C57/BL6 mice (6–8 wk) were purchased from Shanghai Slaccas Experimental Animal Co., Ltd. All animal study protocols were reviewed and approved by the Institutional Animal Care and Use Committee, Soochow University.

Synthesis of 2-[1-(2-Amino-ethoxy)-1-methyl-ethoxy]-ethylamine (AEE). AEE was synthesized as described previously (Scheme 2A).³⁵ Briefly, *N*-(2-hydroxyethyl)-phthalimide (25 g, 1 equiv) was added to benzene (400 mL), and the solution was cooled to 0 °C in an ice bath. 2-Methoxy propene (12.5 mL, 1 equiv) was slowly added into the solution, and *p*-toluenesulfonic acid (234.1 mg, 0.01 equiv) was further added. After being stirred for 1 h at 0 °C, the reaction mixture was heated to evaporate the solvent. When cooled to RT, triethylamine (TEA, 30 mL) and acetic anhydride (7.5 mL) were added, and the mixture was stirred overnight at RT. The crude product was precipitated from the solution using hexanes which was further purified by recrystallization with ethyl acetate for twice to obtain the final product compound **1** as yellow solid (7.8 g, yield 28.9%).

Compound **1** was deprotected in 6 M NaOH (50 mL) at 100 °C overnight. The solution was extracted with CHCl₃/iPrOH (1/1, v/v, 100 mL \times 3) and the organic phase was combined and dried over anhydrous Na₂SO₄. The solution was filtered and concentrated by rotary evaporation. The excess of iPrOH was removed by repeated washing with hexanes and the final product of AEE was obtained as yellow oil (2 g, yield 66.9%).

Synthesis of *N*-[2-[1-(2-Acryloylamino-ethoxy)-1-methyl-ethoxy]-ethyl]-acrylamide (AEA). AEE (0.5 g, 1 equiv) was dissolved in CH₂Cl₂ (20 mL) containing TEA (2.6 mL, 6 equiv) at 0 °C. Acryloyl chloride (0.74 mL, 3 equiv) was slowly added into the solution and the reaction mixture was stirred overnight at room temperature. The solvent was removed by rotary evaporation, and the residue was dissolved in ethyl acetate (100 mL) and washed with 10% (w/v) K₂CO₃ solution (70 mL \times 3). The organic phase was combined and dried over anhydrous Na₂SO₄. Finally, the solution was filtered and concentrated by rotary evaporation to obtain the product AEA as yellow oil (0.25 g, yield 30%).

Synthesis of *N*-(7-Acryloylamino-heptyl)-acrylamide (AHA). AHA as a nonresponsive analogue of AEA was synthesized from 1,7-diaminoheptane instead of AEE by following the same method as described before (Scheme 2B).

Synthesis of Cross-Linked PEI. K-PEI was synthesized via Michael addition reaction of AEA and L-PEI (Scheme 3).³⁰ Briefly, L-PEI (30 mg) was dissolved in methyl alcohol (0.5 mL) and heated to 45 °C in a three-necked flask under a nitrogen atmosphere. AEA (20 mg, molar ratio of acrylate in AEA to primary amine in PEI = 1:2) was dissolved in methyl alcohol (0.5 mL) and added into the L-PEI solution which was stirred in the dark for 48 h under a nitrogen atmosphere. The obtained

polymer was dialyzed against distilled water (pH = 8, MWCO = 1 kDa) for 3 days and lyophilized. The MW of the polymer was determined by MALDI-TOF (Bruker, ultraflex extreme MALDI-TOF/TOF). To enable direct comparison on the pH-responsiveness, cross-linked, non-responsive PEI (NK-PEI) was synthesized from L-PEI and the nonresponsive cross-linker AHA using the same method as described above (Scheme 3). The following nomenclature "K-PEI *a*" was adopted for the cross-linked K-PEI, where *a* represents the molar feed ratio of primary amine (in L-PEI) to acrylate (in AEA) during the Michael addition reaction. The nomenclature of "K-PEI" was used throughout the study to represent K-PEI 2 unless otherwise specified.

Polymer Degradation. K-PEI was dissolved in D₂O (pH 5.0) and incubated at 37 °C for different time before being subjected to ¹H NMR analysis to evaluate polymer degradation. The alteration of polymer MW upon acid (pH 5.0) treatment was also determined by MALDI-TOF.

Preparation and Characterization of Polyplexes. K-PEI and DNA were separately dissolved in DI water at 1 mg/mL. K-PEI was added to DNA at various weight ratios, and the mixture was vortexed for 10 s and incubated at 37 °C for 30 min to allow DNA condensation and formation of the K-PEI/DNA binary polyplexes. HA (1 mg/mL) was then added to the freshly prepared K-PEI/DNA polyplexes at various HA/DNA weight ratios which were incubated at RT for 1 h to allow HA coating and formation of the K-PEI/HA/DNA ternary polyplexes. Freshly prepared polyplexes were also visualized by transmission electron microscopy (TEM) after staining with 1% phosphotungstic acid.

To evaluate the DNA condensation capability, freshly prepared polyplexes were subjected to electrophoresis on a 1% agarose gel at 100 V for 40 min. To quantitatively determine the DNA condensation level, the ethidium bromide (EB) exclusion assay was adopted.³⁶ Briefly, EB solution was added into the polyplexes at the DNA/EB weight ratio of 10:1. After incubation at 37 °C for 1 h, the fluorescence intensity was measured by spectrofluorimetry ($\lambda_{\text{ex}} = 510$ nm, $\lambda_{\text{em}} = 590$ nm). A pure EB solution and the DNA/EB solution without any polymer were used as negative and positive controls, respectively. The DNA condensation efficiency (%) was defined as following:

$$\text{DNA condensation efficiency(\%)} = \left(1 - \frac{F - F_{\text{EB}}}{F_0 - F_{\text{EB}}} \right) \times 100$$

where F_{EB} , F , and F_0 denote the fluorescence intensity of pure EB solution, DNA/EB solution with polymer, and DNA/EB solution without polymer, respectively.

In order to investigate the alteration of the DNA condensation capacity of K-PEI upon acid treatment, pH of the polyplexes was adjusted to 5.0 and the polyplexes were incubated at 37 °C for 4 h before the pH was adjusted back to 7.2. The DNA condensation level of acid-treated polyplexes was evaluated by both the gel retardation assay and EB exclusion assay as described above.

To evaluate the stability of polyplexes in salt and upon dilution, freshly prepared polyplexes were diluted with normal saline (pH 7.2) for 10-fold and incubated with different time before the particle size and zeta potential were monitored by dynamic laser scanning (DLS) on a Malvern Zetasizer. The stability of polyplexes in serum was also studied by addition of serum into the polyplex solution at the final concentration of 10% and incubation at RT for different time before measurement of particle size by DLS. Additionally, particle size and zeta potential of freshly prepared polyplexes and acid-treated polyplexes (pH 5.0 for 4 h) were also monitored to evaluate the pH-responsiveness of polyplexes.

DNA Release. The heparin replacement assay was adopted to evaluate DNA release from polyplexes.³⁷ Briefly, heparin was added to the polyplex solution at various final concentrations and the polyplexes were incubated at 37 °C for 1 h before quantification of the DNA condensation level using the EB exclusion assay as described above. Acid-treated polyplexes (pH 5.0 for 4 h) were also explored to study the pH-responsive DNA release profiles.

In Vitro Transfection. HeLa cells were seeded on 96-well plates at 6×10^3 cells/well and cultured in DMEM containing 10% FBS for 24 h. The medium was changed to opti-MEM (100 μ L/well) into which polyplexes were added at 0.5 μ g DNA/well. After incubation at 37 °C for

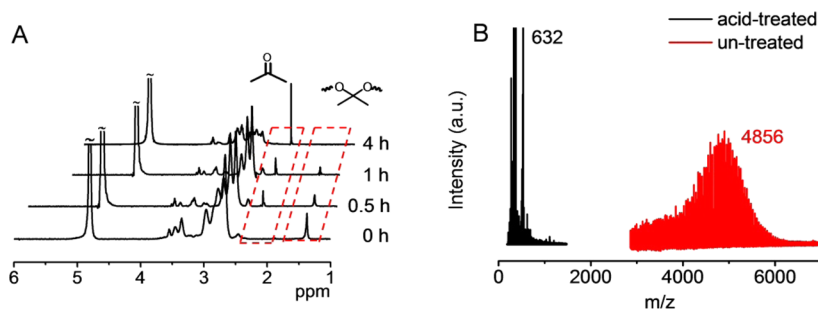


Figure 1. (A) ^1H NMR spectra of K-PEI in D_2O following acid treatment (pH 5.0) for different times. (B) MALDI-TOF spectra of K-PEI before and after acid treatment (pH 5.0, 4 h).

4 h, the medium was replaced by DMEM containing 10% FBS and cells were further incubated for another 20 h. Luciferase expression was quantified in terms of luminescence intensity using a Bright-Glo Luciferase assay kit (Promega), and the cellular protein level was determined using a BCA kit (Pierce). The transfection efficiency was expressed as relative luminescence unit (RLU) associated with 1 mg of cellular protein (RLU/mg protein). In order to study the transfection efficiency of polyplexes in the presence of serum, cells were incubated with polyplexes in DMEM containing 10% FBS for 4 h before refreshment of fresh media and further incubation for 20 h as described above. To evaluate the generality of K-PEI, transfection studies were also performed in different mammalian cell types, as described above, including B16F10, RAW 264.7, and 3T3-L1 cells.

To further probe the HA-assisted targeting effect, cells were pretreated with free HA (final concentration of 10 mg/mL) for 4 h, washed with PBS for three times, and transfected with K-PEI/HA/DNA polyplexes as described above. CD44^+ cells expressing HA receptors (HeLa and B16F10) and CD44^- cells without HA receptors (3T3-L1) were selected for the transfection study.

Intracellular Kinetics. DNA was labeled with YOYO-1 at one dye molecule per 50 bp DNA,³⁸ and the YOYO-1-DNA was allowed to form polyplexes with polymers as described above. Cells were seeded on 96-well plates at 1×10^4 cells/well and cultured for 24 h. The medium was changed to opti-MEM and K-PEI/HA/DNA polyplexes were added at $0.1 \mu\text{g}$ YOYO-1-DNA/well. After incubation at 37°C for 4 h, cells were washed three times with PBS containing heparin (20 U/mL) before being lysed with the RIPA lysis buffer (100 μL /well). YOYO-1-DNA content in the lysate was quantified by spectrofluorimetry ($\lambda_{\text{ex}} = 485 \text{ nm}$, $\lambda_{\text{em}} = 530 \text{ nm}$) and the protein content was measured using the BCA kit. Uptake level was expressed as ng YOYO-1-DNA associated with 1 mg cellular protein. To study the HA-mediated targeting effect of polyplexes, cells were pretreated with free HA (10 mg/mL) for 4 h before addition of the K-PEI/HA/DNA polyplexes. The uptake level of YOYO-1-DNA was quantified 4 h later as described above.

To study the internalization mechanism of the polyplexes, the cellular uptake study was performed at 4°C or in the presence of various endocytic inhibitors. Briefly, cells were preincubated with chlorpromazine (10 $\mu\text{g}/\text{mL}$), genistein (100 $\mu\text{g}/\text{mL}$), methyl- β -cyclodextrin (m β CD, 5 mM), and wortmannin (10 $\mu\text{g}/\text{mL}$) for 30 min prior to polyplex addition and throughout the 4-h uptake experiment at 37°C . Results were expressed as percentage uptake of control cells that were treated with polyplexes at 37°C for 4 h in the absence of inhibitors.

The internalization and intracellular distribution of polyplexes were also visualized by confocal laser scanning microscopy (CLSM). Briefly, HeLa cells were seeded on coverslips in 24-well plate at 3×10^4 cells/well and were cultured for 24 h before treatment with polyplexes in opti-MEM at $1 \mu\text{g}$ YOYO-1-DNA/well for 4 h. Cells were washed three times with heparin-containing PBS, stained with LysoTracker-Red (200 nM), fixed with paraformaldehyde (4%), and stained with DAPI (5 $\mu\text{g}/\text{mL}$) before CLSM observation.

Cytotoxicity. Cells were seeded on 96-well plates at 6×10^3 cells/well and cultured in DMEM containing 10% FBS for 24 h. The polymers were added at various concentrations and incubated for 24 h. Cells without polymer treatment served as the control. Cell viability was

determined by the MTT assay, and results were presented as percentage viability of control cells. To further study the cytotoxicity of polyplexes by simulating the transfection process, cells were incubated with K-PEI/DNA polyplexes prepared at various K-PEI/DNA weight ratios at $0.1 \mu\text{g}$ DNA/well and 37°C for 4 h. The polyplexes were removed, the medium was replaced by fresh DMEM containing 10% FBS, and cells were further incubated for another 20 h. Cell viability was evaluated by the MTT assay as described above. In a parallel study, cells were incubated with K-PEI/HA/DNA polyplexes (K-PEI/DNA weight ratio of 5) at various DNA amount (0.2, 0.6, 1 $\mu\text{g}/\text{well}$) for 4 h, further cultured for 20 h, and subjected to viability assessment using the MTT assay.

In Vivo Transfection. Melanoma-bearing mice were obtained by subcutaneous injection of B16F10 cells. Briefly, male C57/BL6 mice (18–20 g) were un-haired, anesthetized by isoflurane, and subcutaneously injected with 1×10^7 cells in the right flank. When the tumor volume reached 100 mm^3 (within ~ 7 days), mice were divided into six groups (four mice per group), anesthetized, and intratumorally injected with K-PEI/HA/DNA polyplexes, K-PEI/DNA polyplexes, NK-PEI/DNA polyplexes, L-PEI/DNA polyplexes, H-PEI/DNA polyplexes, and HEPES buffer containing 5% glucose (HBG) at $30 \mu\text{g}$ DNA/mouse ($\sim 50 \mu\text{L}/\text{injection}$). Polyplexes were prepared in HBG as described above with minor modifications. Briefly, K-PEI and DNA were separately dissolved in HBG at 20 and 1 mg/mL. K-PEI was added to DNA at weight ratio of 10, and the mixture was vortexed for 10 s and incubated at 37°C for 30 min to allow polyplex formation. HA (20 mg/mL) was then added to the freshly prepared K-PEI/DNA polyplexes at the HA/DNA weight ratio of 5 which were incubated at RT for 1 h to allow HA coating and formation of the K-PEI/HA/DNA ternary polyplexes.

Forty-eight hours post-injection, mice were sacrificed, and tumors were harvested, washed three times with PBS, and homogenized with passive lysis buffer containing protease inhibitor cocktail. The mixture was frozen in liquid nitrogen and thawed in 37°C water bath for three cycles. The mixture was then centrifuged at 4°C and 12000 rpm for 10 min. The supernatant was subjected to quantification of the luciferase expression level using the Bright-Glo assay kit and protein level using the BCA kit. Transfection efficiencies were represented as RLU/mg protein.

Statistical Analysis. Statistical analysis was performed using Student's *t* test. The differences between test and control groups were judged to be significant at $*p < 0.05$ and very significant at $**p < 0.01$ and $***p < 0.001$.

RESULTS AND DISCUSSION

Characterization of Cross-Linked K-PEI. K-PEI was synthesized via the Michael addition between AEA and L-PEI. Ketal-containing cross-linker was selected here to cross-link L-PEI because it had been extensively reported that ketal bond was stable at neutral physiological pH while can be rapidly cleaved at the acidic endosomal pH (~ 5.0). As such, ketone group will be generated and the cross-linked PEI can instantaneously degrade into low-MW segments to promote DNA release and self-diminish the cytotoxicity. As shown in Supporting Information,

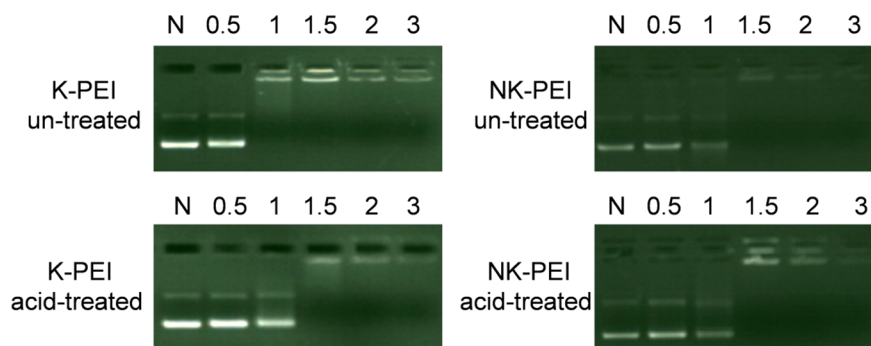


Figure 2. DNA condensation by K-PEI at various polymer/DNA weight ratios and acid-triggered (pH 5.0, 4 h) DNA release as evaluated by the gel retardation assay. N represents naked DNA.

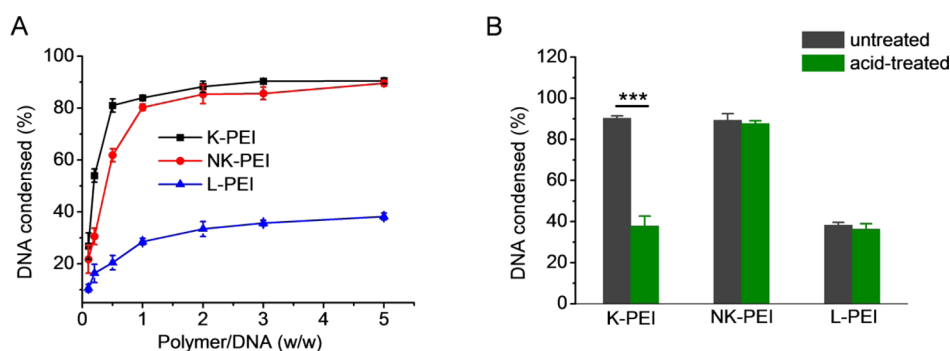


Figure 3. (A) DNA condensation efficiency of K-PEI, NK-PEI, and L-PEI at various polymer/DNA weight ratios as evaluated by the EB exclusion assay ($n = 3$). (B) Alteration of the DNA condensation efficiencies of K-PEI, NK-PEI, and L-PEI following acid treatment (pH 5.0, 4 h). Polymer/DNA weight ratio was maintained constant at 5 ($n = 3$).

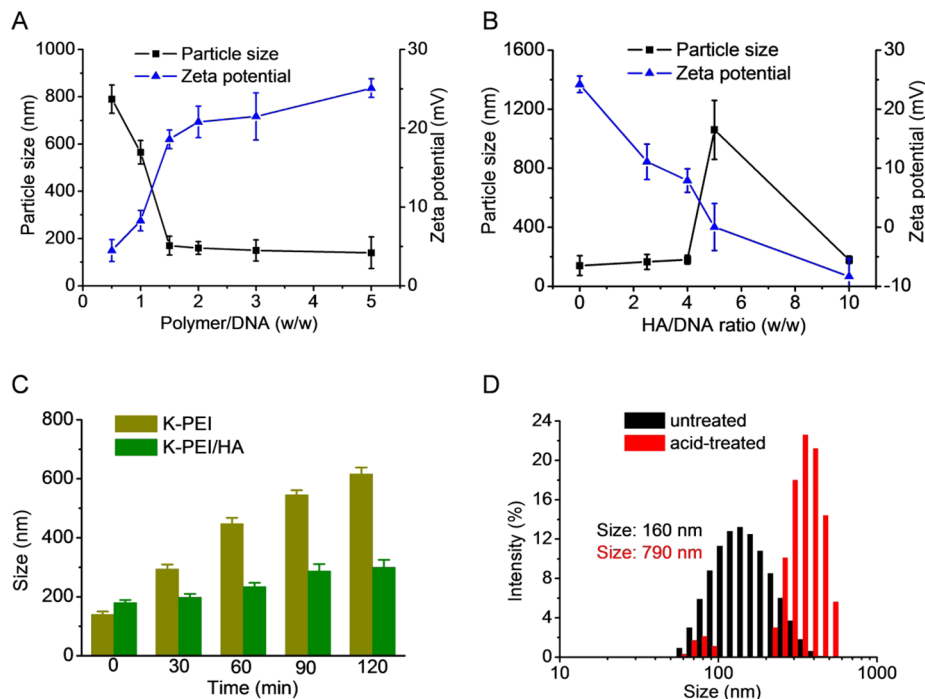


Figure 4. (A) Size and zeta potential of K-PEI/DNA polyplexes at various polymer/DNA weight ratios. (B) Size and zeta potential of K-PEI/HA/DNA polyplexes at various HA/DNA weight ratios. K-PEI/DNA weight ratio was maintained at 5. (C) Alteration of the particle size of K-PEI/DNA polyplexes (weight ratio of 5) and K-PEI/HA/DNA polyplexes (weight ratio of 5/2.5/1) in normal saline. (D) pH-triggered size augmentation of K-PEI/DNA polyplexes (weight ratio of 5) following acid treatment (pH 5.0, 4 h).

Figure S5, the proton peaks of $-NCH_2CH_2-$ in L-PEI (δ 2.5–3.0 ppm) and the proton peaks of the ketal bond (a–c) appeared

while the peaks from acrylate (δ 5.6–6.2 ppm in Supporting Information, Figure S3) disappeared, indicating successful cross-

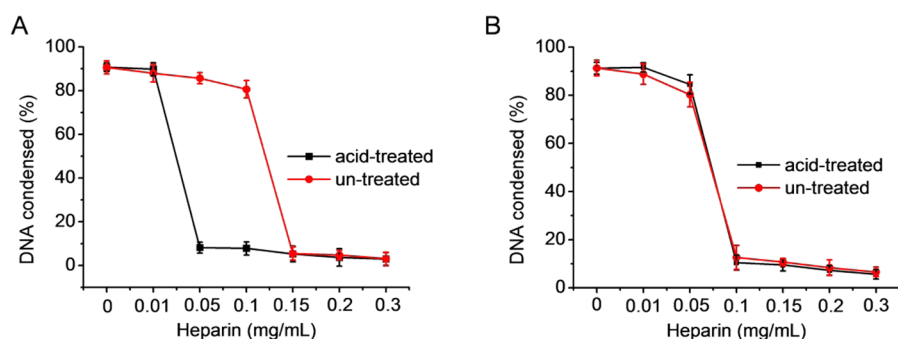


Figure 5. DNA release from K-PEI/DNA polyplexes (A) and NK-PEI/DNA polyplexes (B) in the presence of heparin at various concentration before and after acid (pH 5.0) treatment ($n = 3$).

linking of L-PEI by AEA. MALDI-TOF results revealed that MW of L-PEI increased from 600 to 4856 Da after the Michael addition reaction, indicating formation of high-MW polymer after intermolecular cross-linking.

Polymer Degradation. Acid-triggered polymer degradation was explored using ^1H NMR and MALDI-TOF. Because the endolysosomal pH was similar to 5.0, K-PEI was dissolved in pH 5.0 D_2O and its ^1H NMR spectrum was recorded at different timed intervals. As shown in Figure 1A, the proton peak of the ketal bond at 1.37 ppm gradually disappeared when K-PEI was incubated at pH 5.0 up to 4 h, while the proton peak of the ketone group at 2.2 pm appeared and the peak intensity increased with the incubation time, which demonstrated acid-triggered cleavage of ketal groups and generation of ketone groups. MALDI-TOF further revealed that MW of K-PEI decreased from 4856 to 632 Da that was similar to the MW of non-cross-linked L-PEI upon acid (pH 5.0) treatment for 4 h (Figure 1B). These results collectively indicated that acidic pH triggered cleavage of the pH-responsive ketal bonds in AEA that was used to cross-link L-PEI, and thus, the cross-linked K-PEI with higher MW was degraded into low-MW PEI segments.

DNA Condensation and pH-Responsive DNA Release.

The capacity of K-PEI to condense DNA was first characterized by the gel retardation assay. Compared to L-PEI, K-PEI was able to condense DNA at polymer/DNA weight ratio ≥ 1 , as evidenced by the restricted DNA migration in the loading well (Figure 2 and Supporting Information, Figure S7). In consistence with this qualitative observation, the quantitative EB exclusion assay further revealed that $\sim 90\%$ of the DNA was condensed by K-PEI at polymer/DNA weight ratio higher than 1, while L-PEI afforded low DNA condensation efficiency of below 40% even at high polymer/DNA weight ratio up to 5 (Figure 3A). Such disparity substantiated that the inefficient DNA condensation capacity of L-PEI could be greatly improved via chemical cross-linking that yielded high MW analogues. DLS measurement showed that at K-PEI/DNA weight ratio higher than 1.5, nanoscale polyplexes with diameter of ~ 160 nm and positive surface charge of ~ 20 mV could be obtained (Figure 4A). TEM image showed that K-PEI/DNA polyplexes had a spherical morphology with an average particle size of ~ 140 nm (Supporting Information, Figure S8), which was consistent with the DLS measurement.

Upon treatment with acid (pH 5.0, 4 h), DNA completely migrated in the agarose gel at polymer/DNA weight ratio of 1 (Figure 2) and the DNA condensation efficiency notably dropped from 90.1 to 38.2% (Figure 3B), indicating that the capability of K-PEI to condense DNA was weakened in a pH-responsive manner. In accordance with the polymer degradation

profile, longer time of acid treatment promoted DNA release (Supporting Information, Figure S9). Particle size of the K-PEI/DNA polyplexes greatly enhanced from 160 to 790 nm upon acid treatment (Figure 4D), suggesting dissociation of the nanoscale polyplexes as a result of diminished binding affinity toward DNA that served as the driving force for polyplex formation.

In support of the above assessment on the pH-responsiveness of K-PEI, the DNA condensation efficiency of NK-PEI, a nonresponsive analogue of K-PEI which formed polyplexes with similar diameter and positive surface charge to K-PEI (Supporting Information, Figure S10), did not change upon acid treatment (Figure 3B), which further substantiated that acid-induced ketal cleavage contributed to the degradation of K-PEI and accordingly promoted DNA dissociation.

When K-PEI/DNA polyplexes were coated with HA to form ternary complexes, the DNA condensation level did not appreciably change except the slight decrease at the HA/DNA weight ratio of 10 (Supporting Information, Figure S11). This could be attributed to the excessive amount of negatively charged HA that competitively reduced the electrostatic interactions between K-PEI and DNA and accordingly partly replaced DNA out of the polyplexes. At the HA/DNA weight ratio lower than 4, size of the K-PEI/HA/DNA ternary polyplexes remained around 200 nm and showed no significant difference to the K-PEI/DNA binary polyplexes (Figure 4B). However, further increase in the HA coating amount led to dramatic elevation of particle size up to ~ 1000 nm, which was mainly attributed to the neutralization of the positive surface charge of polyplexes by the negatively charged HA as evidenced by the continuously reduced zeta potential that led to particle aggregation (Figure 4B). Further increase in the HA amount led to complete coating of polyplex surface with the anionic HA molecules, leading to negative surface charge and accordingly improved particle dispersion due to the electrostatic repulsion among each other.

Stability of polyplexes in salt solution or 10% serum was further evaluated in terms of particle size alteration. As shown in Figure 4C, particle size of K-PEI/DNA binary polyplexes dramatically increased upon dilution with normal saline while size of the K-PEI/HA/DNA ternary polyplexes were only slightly increased to ~ 280 nm within 2 h. Similar results were observed after incubation with 10% serum (Supporting Information, Figure S12), indicating that HA coating significantly improved the stability of polyplexes against salt and dilution. As a negatively charged polysaccharide, HA absorbed water and formed a hydrophilic corona on polyplexes surface to reduce the “charge shielding” effect induced by the salt in the solution. As such, the polyplex stability was greatly improved, and the obtained K-PEI/

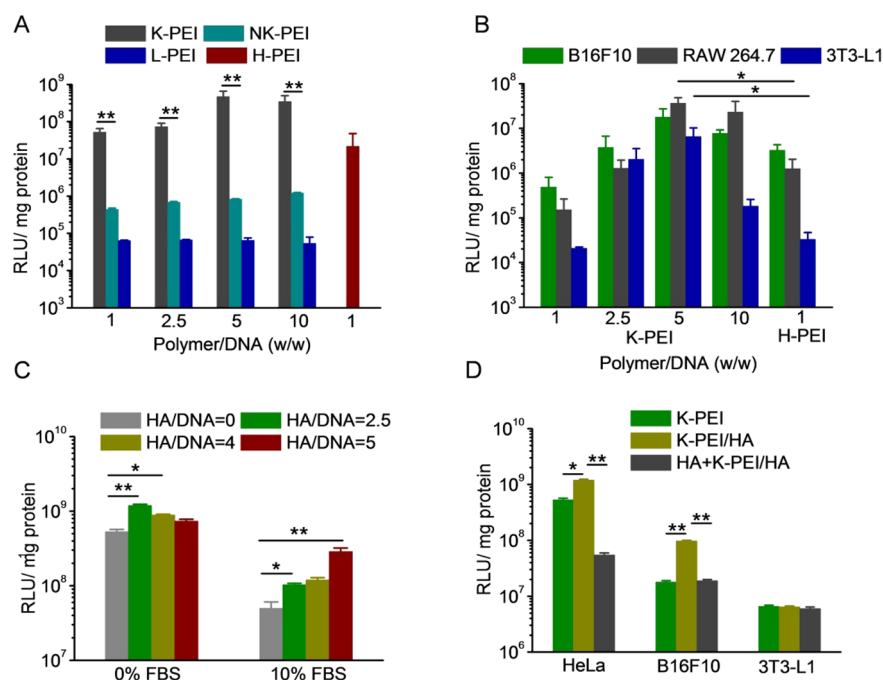


Figure 6. (A) Comparison of the transfection efficiencies K-PEI, NK-PEI, L-PEI, and H-PEI in HeLa cells in the absence of serum ($n = 3$). (B) Transfection efficiencies of K-PEI in B16F10, RAW 264.7, and 3T3-L1 cells in the absence of serum ($n = 3$). (C) Transfection efficiencies of K-PEI/HA/DNA polyplexes in HeLa cells in the absence or presence of serum ($n = 3$). K-PEI/DNA weight ratio was maintained constant at 5. (D) Transfection efficiencies of K-PEI/DNA and K-PEI/HA/DNA polyplexes (weight ratio of 5/2.5/1) in HeLa, B16F10, and 3T3-L1 cells in the absence of serum with or without pretreatment of free HA ($n = 3$). H-PEI was used as a control at the optimal polymer/DNA weight ratio of 1 in the above assessments.

HA/DNA ternary complexes may be more suitable for *in vivo* use.

To reflect the intracellular DNA release in the presence of anionic polysaccharides/proteins, the acid-triggered DNA unpacking was also monitored using the heparin replacement assay. As shown in Figure 5A, DNA was released from K-PEI/DNA polyplexes in the presence of 0.15 mg/mL heparin. Comparatively, a 3-fold lower concentration (0.05 mg/mL) of heparin was required to release DNA from acid-triggered K-PEI polyplexes, suggesting promoted DNA dissociation as a result of acid-triggered degradation of K-PEI. The heparin-induced DNA release profiles of the nonresponsive NK-PEI did not appreciably alter upon acid treatment (Figure 5B). These results collectively substantiated our design strategy to promote “on-demand” DNA release by cascading instantaneous polymer degradation in response to the endolysosomal acidic pH.

In Vitro Transfection. The transfection efficiencies of polyplexes were first evaluated in HeLa cells under serum-free condition. A spectrum of K-PEI synthesized at different primary amine (L-PEI)/acrylate (cross-linker) molar ratios was screened, and K-PEI 2 at the polymer/DNA weight ratio of 5 turned out to display the highest transfection efficiency (Supporting Information, Figure S13). Therefore, it was selected as the top-performing material to further evaluate the pH-responsive gene transfection capabilities. As illustrated in Figure 6A, K-PEI polyplexes showed remarkably higher transfection efficiency than NK-PEI and L-PEI by 2–3 orders of magnitude. In direct comparison with H-PEI as the benchmark positive control, a 20-fold higher transfection efficiency was also noted at the optimal K-PEI/DNA and H-PEI/DNA weight ratios of 5 and 1, respectively.

The superiority and generality of K-PEI in mediating effective gene transfection was also demonstrated in another three mammalian cell types, including B16F10 (melanoma cells),

RAW 264.7 (macrophage), and 3T3-L1 (primary fibroblast), wherein K-PEI again showed a 1–2 order of magnitude higher transfection efficiencies than H-PEI (Figure 6B). These results thus substantiated that cross-linking of L-PEI to form high-MW K-PEI and acid-triggered de-cross-linking of K-PEI at endolysosomal pH greatly potentiated the DNA transfection capabilities by facilitating DNA condensation in the extracellular compartment while promoting intracellular DNA release.

Cancer cells express HA receptors (CD44⁺) on cell membranes, and thus, surface coating of HA should lead to active targeting to cancer cells. As such, the transfection efficiencies of HA-coated polyplexes were further evaluated in CD44⁺ cancer cells. As shown in Figure 6C, K-PEI/HA/DNA polyplexes (HA/DNA weight ratio of 2.5) showed a 2.5-fold higher transfection efficiency than K-PEI/DNA polyplexes in HeLa cells. Similar enhancement was also noted in B16F10 cells (CD44⁺) but not in 3T3-L1 cells (CD44⁻), which thus substantiated the HA-mediated targeting effect to potentiate gene transfection in cancer cells. When HeLa and B16F10 cells were pretreated with HA to competitively block the HA receptors on cell membranes, the transfection efficiency of K-PEI/HA/DNA ternary polyplexes dramatically decreased (Figure 6D), which further confirmed that the augmented transfection efficiency of ternary polyplexes was related to the HA-mediated targeting effect. 3T3-L1 does not express HA receptors, and thus pretreatment with HA did not lead to appreciable effect on the transfection efficiency.

Remarkably compromised transfection efficiency by serum is a major challenge for polycation-based nonviral gene vectors especially when used *in vivo*. We thus further evaluated the gene transfection efficiencies of polyplexes in HeLa cells in the presence of 10% serum. As depicted in Supporting Information, Figure S14, the transfection efficiency of K-PEI was slightly reduced by several fold compared to that under serum-free

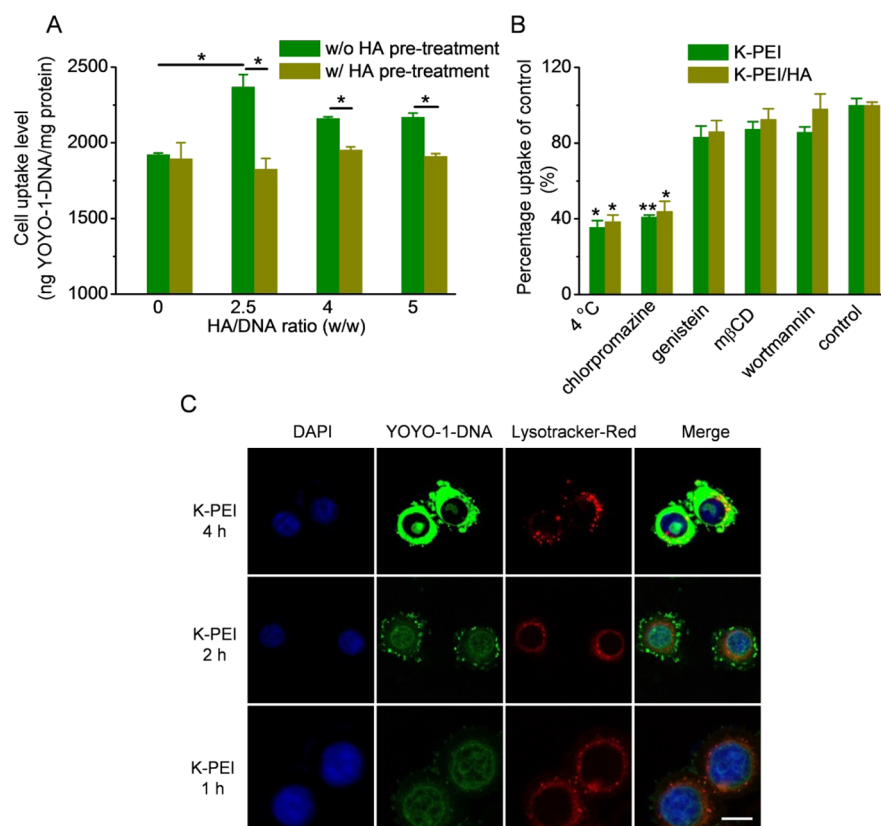


Figure 7. Intracellular kinetics of polyplexes in HeLa cells. (A) Uptake level of K-PEI/HA/DNA polyplexes containing YOYO-1-DNA in HeLa cells with or without pretreatment of HA following incubation at 37 °C for 4 h. K-PEI/DNA weight ratio was maintained constant at 5 ($n = 3$). (B) Uptake level of K-PEI/DNA polyplexes (weight ratio of 5/1) and K-PEI/HA/DNA polyplexes (weight ratio of 5/2.5/1) at 4 °C or in the presence of various endocytic inhibitors ($n = 3$). (C) CLSM images of HeLa cells following incubation with K-PEI/HA/YOYO-1-DNA polyplexes at 37 °C for 1, 2, and 4 h. Cell nuclei were stained with DAPI and endosomes/lysosomes were stained with Lysotracker-Red. Bar represents 15 μm .

condition, and a 10-fold higher transfection efficiency was still noted when compared to H-PEI, which collectively demonstrated the superiority of cross-linked K-PEI under the serum-containing condition. Comparatively, the K-PEI/HA/DNA ternary polyplexes (HA/DNA weight ratio of 5) achieved comparable transfection efficiency to that under serum-free condition (Supporting Information, Figure S15). Such results indicated that HA coating greatly enhanced the capability of polyplexes to resist serum, mainly because HA reduced the affinity between polyplexes and serum protein and thus greatly enhanced the polyplexes stability. The desired serum-resistance of HA-coated ternary polyplexes indicated their promising potential for *in vivo* gene delivery.

Intracellular Kinetics. The gene transfection efficiencies of nonviral vectors are closely related to their intracellular kinetics and internalization pathways. Therefore, the cell uptake level and internalization mechanisms of K-PEI polyplexes were explored. As shown in Supporting Information, Figure S16, K-PEI notably promoted the internalization of DNA at polymer/DNA weight ratios of 2.5–10 and the cell uptake level increased with the incubation time. In direct comparison with H-PEI and L-PEI, a 3–5-fold increment in terms of the cell uptake level was also noted. In consistence with the transfection efficiency, HA-coated ternary polyplexes exhibited a 2-fold higher cell uptake level than the binary polyplexes via HA-receptor-mediated cancer cell targeting and internalization. Pretreatment of HeLa cells with free HA significantly reduced the cell uptake level of ternary

polyplexes, which again substantiated the HA-mediated targeting effect (Figure 7A).

The internalization pathway of the polyplexes was then probed by lowering the temperature or using different endocytic inhibitors. Energy-dependent endocytosis is blocked at low temperature (4 °C); chlorpromazine inhibits the clathrin-mediated endocytosis (CME) by inducing the dissociation of the clathrin lattice; genistein and mβCD inhibit caveolae by inhibiting tyrosine kinase and depleting cholesterol, respectively; wortmannin prevents micropinocytosis by inhibiting phosphatidylinositol-3-phosphate.^{38,39} As shown in Figure 7B, the cell uptake level was significantly decreased by 60% at 4 °C, suggesting that the majority of the polyplexes entered the cell through energy-dependent endocytosis while the remaining may be physical adhesion or diffusion. The cell uptake level also was significantly inhibited by chlorpromazine but not genistein, mβCD or wortmannin, indicating that the polyplexes were internalized mainly via CME rather than caveolae or micropinocytosis. We further studied the internalization pathway of the polyplexes in B16F10 and RAW 264.7 cells (Supporting Information, Figure S17). The cell uptake level was significantly inhibited by chlorpromazine in B16F10 cells and by wortmannin in RAW 264.7 cells, which indicated that the polyplexes were internalized mainly via CME in B16F10 cells and micropinocytosis in RAW 264.7 cells.

Endosomal entrapment and lysosomal degradation of the gene cargoes serve as a critical barrier against effective nonviral gene delivery. Therefore, the capability of K-PEI polyplexes to avoid/

escape endosomes/lysosomes was further studied. CLSM images revealed that polyplexes were effectively taken up by HeLa cells as evidenced by extensive cytoplasmic distribution of YOYO-1-DNA post 4-h incubation (Figure 7C), and green fluorescence (YOYO-1-DNA) greatly separated from red fluorescence of LysoTracker-red-stained endosomes/lysosomes (Figure 7C), which demonstrated that K-PEI was able to effectively avoid endosomal/lysosomal entrapment due to the “proton sponge” effect mediated by the amine groups on K-PEI (Scheme 1). YOYO-1-DNA was also noted to be distributed in DAPI-stained nuclei, which indicated that it can be effectively transported into the nuclei where gene transcription was initiated.

Cytotoxicity. Transfection efficiency and cytotoxicity of polycations are often inversely correlated. For instance, polycations with higher MW often afford stronger DNA condensation capacities and higher transfection efficiencies than their low-MW analogues. However, at the same time, polycations with higher MW also induce higher cytotoxicities than their low-MW analogues that are much easier to be expelled from the biological membranes because of fewer contact points with the cell components for each individual polymeric chain. The excessive cytotoxicities especially at high doses will lead to irreversible damage to target cells and ultimately impair the transfection efficiencies. To this end, it is ideal that the polycation vector possess high MW before transfection to enable effective DNA condensation and intracellular delivery, while degrade into small segments post-transfection to diminish the material toxicity. As shown in Figure 8A, H-PEI that is widely used as a golden standard nonviral transfection reagent induced notable cytotoxicities when the concentration reached up to 0.05 mg/mL. Acid-treated NK-PEI showed appreciable cytotoxicity, which could be attributed to its relatively high MW after cross-linking and inability to degrade into low-MW segments upon acid treatment. In comparison, acid-treated K-PEI showed significantly lower cytotoxicity comparable to that of the L-PEI after long-term (24 h) incubation, indicating that acid-triggered degradation of K-PEI effectively contributed to the self-diminishment of material toxicity. It was also noted that the cytotoxicity of K-PEI was dramatically reduced upon acid pretreatment while that of NK-PEI did not appreciably change (data not shown), which served as an evidence for the acid-triggered self-diminishment of the cytotoxicity of K-PEI.

To reflect the transfection process and explore the effect of endolysosomal acidic pH on the cytotoxicity of K-PEI, polyplexes were formed and incubated with cells for 4 h before further incubation for 20 h and assessment of cell viability. As shown in Figure 8B, K-PEI polyplexes showed notably lower cytotoxicities than NK-PEI polyplexes at all test polymer/DNA weight ratios, and the desired cell tolerance of K-PEI polyplexes (viability above 90%) was comparable to that of the L-PEI polyplexes. These findings thus demonstrated our proposed design strategy to eliminate the long-term cytotoxicity of PEI by self-reduction of the MW via endolysosomal pH-triggered de-cross-linking. HA coating on polyplexes further reduced the material toxicity, and higher amount of HA corresponded to elevated cell viability, which could be attributed to the reduction of surface positive charge density of polyplexes and formation of a hydrophilic outer shell (Figure 8C).

In Vivo Transfection. We further evaluated the in vivo transfection efficiencies of polyplexes in melanoma-bearing CS7/BL6 mice following intratumoral injection to explore the potential of K-PEI/HA/DNA ternary polyplexes for in vivo gene delivery. In consistence with the in vitro results, K-PEI/

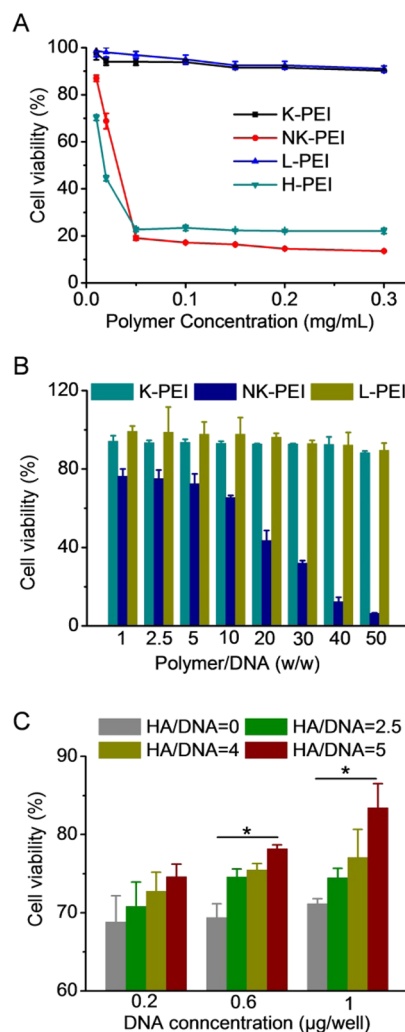


Figure 8. Cytotoxicity of acid-pretreated free polymer following 24 h incubation (A), polymer/DNA polyplexes following 4 h incubation (B), and HA-coated K-PEI/DNA polyplexes, following 4 h incubation at various HA/DNA weight ratios (C) in HeLa cells as determined by the MTT assay ($n = 3$).

HA/DNA polyplexes showed a 2-fold higher transfection efficiency than K-PEI/DNA polyplexes which was 1–2 orders of magnitude higher than those of H-PEI and L-PEI polyplexes, respectively (Figure 9). These results suggested the potential utilities of K-PEI/HA/DNA ternary polyplexes for the topical

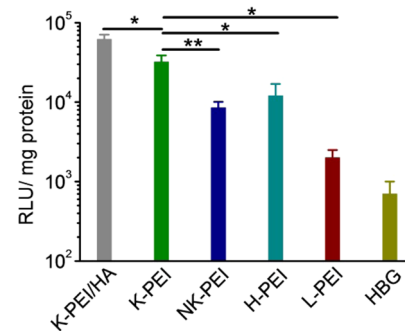


Figure 9. In vivo transfection efficiencies of polyplexes following intratumoral injection in B16F10 xenograft tumor-bearing mice at 30 μg DNA/mouse ($n = 4$).

DNA delivery toward cancer gene therapy, and they again substantiated our design strategy to potentiate the transfection efficiencies of polycations via polyanion-assisted cancer targeting and cleavable cross-linking that is amenable to degradation in response to internal triggers (such as acidic pH in the endolysosomes).

CONCLUSIONS

In summary, we designed a strategy to promote the intracellular DNA release as well as reduce the polycation toxicity by reversibly cross-linking low-MW PEI with acid-labile linkers. By coating the polyplexes with HA, we were able to enhance the stability of polyplexes, further reduce the material toxicity, and strengthen the transfection efficiencies in cancer cells in vitro and in vivo via HA-receptor-mediated cancer targeting. With the collective contribution of HA-promoted cancer cell internalization and acid-promoted polymer degradation, the obtained K-PEI/HA/DNA ternary polyplexes exhibited notably enhanced transfection efficiencies by 1–2 orders of magnitude and greatly diminished cytotoxicity compared to PEI 25 kDa as the golden standard transfection reagent. This study thus provides an effective approach to address the efficiency-toxicity inconsistency of polycation-based gene vectors, and the pH-responsive, cancer-targeting K-PEI/HA/DNA polyplexes hold great promises for cancer gene therapy.

ASSOCIATED CONTENT

Supporting Information

¹H NMR spectra of cross-linkers and cross-linked polymers, DLS measurement of NK-PEI/DNA polyplexes, DNA condensation efficiency of ternary complexes, and transfection efficiencies of various K-PEIs in the absence of presence of serum. This material is available free of charge via the Internet at <http://pubs.acs.org>.

AUTHOR INFORMATION

Corresponding Authors

*E-mail: lcyin@suda.edu.cn. Phone: 86-512-65882039.

*E-mail: zyzhong@suda.edu.cn. Phone: 86-512-65880098.

Notes

The authors declare no competing financial interest.

ACKNOWLEDGMENTS

The authors acknowledge the financial support from the National Natural Science Foundation of China (51403145), the Science and Technology Department of Jiangsu Province (BK20140333), and the Collaborative Innovation Center of Suzhou, Nano Science and Technology.

REFERENCES

- (1) Candolfi, M.; Xiong, W.; Yagiz, K.; Liu, C.; Muhammad, A.; Puntel, M.; Foulad, D.; Zadmehr, A.; Ahlzadeh, G. E.; Kroeger, K. M. *Proc. Natl. Acad. Sci. U.S.A.* **2010**, *107*, 20021–20026.
- (2) Wang, J.; Tang, G.; Shen, J.; Hu, Q.; Xu, F.; Wang, Q.; Li, Z.; Yang, W. *Biomaterials* **2012**, *33*, 4597–4607.
- (3) Kay, M. A.; Glorioso, J. C.; Naldini, L. *Nat. Med.* **2001**, *7*, 33–40.
- (4) Mintzer, M. A.; Simanek, E. E. *Chem. Rev.* **2008**, *109*, 259–302.
- (5) Elsbahy, M.; Nazarali, A.; Foldvari, M. *Curr. Drug Delivery* **2011**, *8*, 235–244.
- (6) Zhao, X.; Yin, L.; Ding, J.; Tang, C.; Gu, S.; Yin, C.; Mao, Y. *J. Controlled Release* **2010**, *144*, 46–54.
- (7) Teo, P. Y.; Yang, C.; Hedrick, J. L.; Engler, A. C.; Coady, D. J.; Ghaem-Maghani, S.; George, A. J.; Yang, Y. *Biomaterials* **2013**, *34*, 7971–7979.

- (8) Song, Y.; Wang, H.; Zeng, X.; Sun, Y.; Zhang, X.; Zhou, J.; Zhang, L. *Bioconjugate Chem.* **2010**, *21*, 1271–1279.
- (9) Yin, L.; Ding, J.; He, C.; Cui, L.; Tang, C.; Yin, C. *Biomaterials* **2009**, *30*, 5691–5700.
- (10) Shim, M. S.; Kwon, Y. J. *J. Controlled Release* **2009**, *133*, 206–213.
- (11) Wang, Y.; Zheng, M.; Meng, F.; Zhang, J.; Peng, R.; Zhong, Z. *Biomacromolecules* **2011**, *12*, 1032–1040.
- (12) Zheng, M.; Zhong, Y.; Meng, F.; Peng, R.; Zhong, Z. *Mol. Pharmaceutics* **2011**, *8*, 2434–2443.
- (13) Seib, F. P.; Jones, A. T.; Duncan, R. J. *Controlled Release* **2007**, *117*, 291–300.
- (14) Chollet, P.; Favrot, M. C.; Hurbin, A.; Coll, J. L. *J. Gene Med.* **2002**, *4*, 84–91.
- (15) Brannon-Peppas, L.; Blanchette, J. O. *Adv. Drug Delivery Rev.* **2012**, *64*, 206–212.
- (16) Wang, Y.; Zhu, Y.; Hu, Q.; Shen, J. *Acta Biomater.* **2008**, *4*, 1235–1243.
- (17) Shim, M. S.; Kwon, Y. J. *Adv. Drug Delivery Rev.* **2012**, *64*, 1046–1059.
- (18) Orig, M.; Brunner, S.; Schuller, S.; Kircheis, R.; Wagner, E. *Gene Ther.* **1999**, *6*, 595–605.
- (19) Gebhart, C. L.; Sriadibhatla, S.; Vinogradov, S.; Lemieux, P.; Alakhov, V.; Kabanov, A. V. *Bioconjugate Chem.* **2002**, *13*, 937–944.
- (20) Wang, Y.; Chen, P.; Shen, J. *Colloids Surf., B* **2007**, *58*, 188–196.
- (21) Hatakeyama, H.; Akita, H.; Harashima, H. *Adv. Drug Delivery Rev.* **2011**, *63*, 152–160.
- (22) Hong, R.-L.; Huang, C.-J.; Tseng, Y.-L.; Pang, V. F.; Chen, S.-T.; Liu, J.-J.; Chang, F.-H. *Clin. Cancer Res.* **1999**, *5*, 3645–3652.
- (23) Lammers, T.; Hennink, W.; Storm, G. *Br. J. Cancer* **2008**, *99*, 392–397.
- (24) Akinc, A.; Thomas, M.; Klivanov, A. M.; Langer, R. *J. Gene Med.* **2005**, *7*, 657–663.
- (25) Neu, M.; Germershaus, O.; Behe, M.; Kissel, T. *J. Controlled Release* **2007**, *124*, 69–80.
- (26) Tripathi, S. K.; Gupta, N.; Mahato, M.; Gupta, K. C.; Kumar, P. *Colloids Surf., B* **2014**, *115*, 79–85.
- (27) Yeh, P.-H.; Sun, J.-S.; Wu, H.-C.; Hwang, L.-H.; Wang, T.-W. *RSC Adv.* **2013**, *3*, 12922–12932.
- (28) Xiang, S.; Su, J.; Tong, H.; Yang, F.; Tong, W.; Yuan, W.; Wu, F.; Wang, C.; Jin, T.; Dai, K. *Biomaterials* **2012**, *33*, 6520–6532.
- (29) Lee, S. J.; Min, K. H.; Lee, H. J.; Koo, A. N.; Rim, H. P.; Jeon, B. J.; Jeong, S. Y.; Heo, J. S.; Lee, S. C. *Biomacromolecules* **2011**, *12*, 1224–1233.
- (30) Sun, Y.-X.; Zeng, X.; Meng, Q.-F.; Zhang, X.-Z.; Cheng, S.-X.; Zhuo, R.-X. *Biomaterials* **2008**, *29*, 4356–4365.
- (31) Knorr, V.; Ogris, M.; Wagner, E. *Pharm. Res.* **2008**, *25*, 2937–2945.
- (32) Ito, T.; Iida-Tanaka, N.; Koyama, Y. *J. Drug Target.* **2008**, *16*, 276–281.
- (33) Kim, T. G.; Lee, Y.; Park, T. G. *Int. J. Pharm.* **2010**, *384*, 181–188.
- (34) Jiang, G.; Park, K.; Kim, J.; Kim, K. S.; Hahn, S. K. *Mol. Pharmaceutics* **2009**, *6*, 727–737.
- (35) Paramonov, S. E.; Bachelder, E. M.; Beaudette, T. T.; Standley, S. M.; Lee, C. C.; Dashe, J.; Fréchet, J. M. *Bioconjugate Chem.* **2008**, *19*, 911–919.
- (36) Deng, X.; Zheng, N.; Song, Z.; Yin, L.; Cheng, J. *Biomaterials* **2014**, *35*, 5006–5015.
- (37) Yin, L.; Tang, H.; Kim, K. H.; Zheng, N.; Song, Z.; Gabrielson, N. P.; Lu, H.; Cheng, J. *Angew. Chem., Int. Ed.* **2013**, *52*, 9182–9186.
- (38) Yin, L.; Song, Z.; Kim, K. H.; Zheng, N.; Tang, H.; Lu, H.; Gabrielson, N.; Cheng, J. *Biomaterials* **2013**, *34*, 2340–2349.
- (39) HoonáKim, K. *Chem. Sci.* **2013**, *4*, 3839–3844.